MDPI

Abstract

Total Focusing In The Virtual Wave Domain: 3D Defect Reconstruction Using Spatially Structured Laser Heating

Julien Lecompagnon [1,*], Ludwig Rooch [1,2], Christian Hassenstein [1], and Mathias Ziegler [1]

[1] Bundesanstalt für Materialforschung und -prüfung (BAM), Division 8.3: Thermographic Methods, Unter den Eichen 87, 12205 Berlin, Germany
[2] Technische Universität Berlin, Straße des 17. Juni 136, Institute of Mathematics, Scientific Computing group, 10587 Berlin, Germany
* Correspondence: julien.lecompagnon@bam.de

Abstract: Classical active thermographic testing of industrial goods has mostly been limited to generating 2D defect maps. While for surface or near-surface defect detection, this is a desired result, for deeply buried defects, a 3D reconstruction of the defect geometry is coveted. This general trend can also be well observed in widely used NDT methods (radiography, ultrasonic testing), where the progression from 2D to 3D reconstruction methods has already made profound progress (CT, UT phased array transducers). Achieving a fully 3D defect reconstruction in active thermographic testing suffers heavily from the diffusive nature of thermal processes. One possible solution to deal with thermal diffusion is the application of the virtual wave concept, which, by solving an inverse problem, allows to extract the diffusiveness from the thermographic data in the post-processing stage. What is left follows propagating wave physics, enabling the usage of well-known algorithms from ultrasonic testing. In this work, we present our progress in the 3D reconstruction of deeply buried defects using spatially structured laser heating in conjunction with applying the well-known total focusing method (TFM) in the virtual wave domain.

Keywords: Non-destructive Testing; Virtual Wave Concept; Laser Thermography; Thermal Thomography

1. Introduction

Active thermographic testing, as a non-destructive testing method, being non-contact and covering large areas at a reasonable speed, offers a unique set of advantages over other non-destructive testing methods. However, one of its main drawbacks is the diffusive nature of thermal processes, which makes it difficult to detect and reconstruct deeply buried defects. Furthermore, in its application highly ill-posed inverse problems arise as usually the Object under Test (OuT) can only be excited at its surfaces, and the temperature response is measured at the surface as well. Achieving a fully 3D tomographic reconstruction of defects — a much sought-after result — is therefore a challenging task for active thermographic testing. In this work, we present our progress towards achieving this goal by combining multiple spatially structured laser heatings with the total focusing method (TFM) known from ultrasonic testing in the virtual wave domain.

2. Methodology

Burgholzer et al. [1] developed a virtual wave concept that connects the diffusive heat equation with the propagating wave equation for ultrasound waves. The result is a

Published:

Citation: Lecompagnon, J.; Rooch, L.; Hassenstein, C.; Ziegler, M. Total Focusing In The Virtual Wave Domain: 3D Defect Reconstruction Using Spatially Structured Laser Heating. *Proceedings* **2025**, *1*, 0. https://doi.org/

Fredholm integral relationship that allows the computation of the virtual wave field T_{virt} based on a known temperature distribution T. The formal equation is given by

$$\begin{aligned} T(\mathbf{r},t) &= \int_{-\infty}^{\infty} T_{\text{virt}}(\mathbf{r},t')K(t,t')\,\mathrm{d}t' \quad , \\ K(t,t') &= \frac{c}{\sqrt{\pi\alpha t}}\exp\left(-\frac{c^2t'^2}{4\alpha t}\right) \quad \text{for } t>0 \quad , \end{aligned} \tag{1}$$

with $\mathbf{r}$ being the position vector and t and t' being the different time scales in time and virtual wave domain. The kernel $K(t,t')$ transforms between both domains and contains the thermal diffusivity α and the virtual speed of sound c as parameters. The corresponding discretized version of Equation 1 for two spatial dimensions x and y is $T = \mathbf{K}T_{\text{virt}}$, where $T \in \mathbb{R}^{N_t\times N_x\times N_y}$ is the observed temperature data, $\mathbf{K} \in \mathbb{R}^{N_t\times N_{t'}}$ is the discretised kernel and $T_{\text{virt}} \in \mathbb{R}^{N_{t'}\times N_x\times N_y}$ is the virtual wave field. The entries of the discrete kernel $\mathbf{K} = \left[K_{i,j}\right] \in \mathbb{R}^{N_t\times N_{t'}}$ can be calculated with

$$K_{i,j} = \frac{\tilde{c}}{\sqrt{\pi\tilde{\alpha}i}}\exp\left(-\frac{\tilde{c}^2(j-1)^2}{4\tilde{\alpha}i}\right) \quad \text{, where} \quad \tilde{c} = c\frac{\Delta_t}{\Delta_z} \quad \text{and} \quad \tilde{\alpha} = \alpha\frac{\Delta_{t'}}{\Delta_z^2} \quad . \tag{2}$$

Here $\Delta_t, \Delta_{t'}$ and Δ_z are the increments of the time, virtual time, and depth vector. The kernel $\mathbf{K}$ is highly rank deficient, which makes solving for T_{virt} non-trivial. To solve this ill-posed inverse problem, we apply the alternating direction method of multipliers (ADMM) [2]. The minimization problem version of the discretized problem is given by [3, Chapter 6.4] as

$$\min_{T_{\text{virt}}} \ \frac{1}{2}\left\|\mathbf{K}T_{\text{virt}} - T\right\|_2^2 + \lambda\left\|T_{\text{virt}}\right\|_1 \quad . \tag{3}$$

Since an ultrasound field is naturally very sparse, it makes sense to incorporate sparsity as an additional constraint into the minimization problem. The sparsity of the solution is achieved by the $\ell 1$-norm of T_{virt} and controlled by the parameter λ, which has to be determined empirically.

Total Focusing Method

The Total Focussing Method (TFM) is a well-established image reconstruction technique for ultrasonic testing [4]. Combined with an full matrix capture (FMC) experimental approach, the method relies on taking multiple measurements of the same OuT with different transmitter positions for each measurement while recording the response using multiple receivers. The transfer to an application within thermographic testing is very natural, as an infrared camera usually records a large region of interest (ROI) at all times, providing a high phase-coherent receiver count. Hence, only a change in the structure of the excitation is necessary for TFM application. This can be facilitated by step-scanning with a single laser spot of any shape [5] or using a full-scale light modulator [6]. Enough cooling time between excitations is necessary to guarantee sufficient independence of all measurements. Given N_{meas} two-dimensional virtual wave fields $T_{\text{virt}} \in \mathbb{R}^{N_{t'}\times N_x\times N_y\times N_{\text{meas}}}$, we can compute the TFM reconstruction result using the following equation:

$$T_{\text{rec}}(P) = \sum_{n=1}^{N_{\text{meas}}}\sum_{P_{tx}}\sum_{P_{rx}} T_{\text{virt}}(t_{tx,rx}(P_{tx,j},P,P_{rx,i}),P_{rx,i},n) \quad , \tag{4}$$

where $P = (x,y,z) \in \mathbb{R}^3$ is the location of a volume element within the discretized OuT, $P_{rx,i} = (x_{rx,i},y_{rx,i}) \in \mathbb{R}^2$ is the location of the i-th receiver and $P_{tx,j} = (x_{tx,j},y_{tx,j}) \in \mathbb{R}^2$ is the location of the j-th transmitter. $t_{tx,rx}$ describes the travel time of the virtual wave from the transmitter $P_{tx,j}$ via the volume element at P to the receiver $P_{rx,i}$.

Using a Euclidean distance function between two points $d(P_1, P_2) = \|P_2 - P_1\|_2$ and the virtual wave speed c, the travel time $t_{tx,rx}$ of the virtual wave can be determined as $t_{tx,rx}(P_{tx}, P, P_{rx}) = (d(P_{tx}, P) + d(P, P_{rx}))/c$.

3. Experimental Setup

The experimental setup is shown in Figure 1. Here, an OuT is examined that has been additively manufactured from stainless steel (316L, 1.4404, $\alpha = 3.5\,\mathrm{mm^2\,s^{-1}}$) and features a height and width of 58.5 mm and a thickness of 4.5 mm. It contains four defect pairs (2 mm × 2 mm rectangular channels) where the gaps between the two defects of each pair are each doubling from 0.5 mm to 4 mm. The OuT is symmetric in the y-direction as the channels run through the whole width. On this OuT, $N_{\mathrm{meas}} = 121$ line excitations for $t_{\mathrm{pulse}} = 300\,\mathrm{ms}$ at $P = 90\,\mathrm{W}$ have been performed using a laser line with a width of 0.38 mm and a step-over of 0.4 mm in the x-direction. The resulting temperature response has been measured using an MWIR cooled infrared camera with a pixel resolution of $\Delta x, \Delta y = 53\,\mu\mathrm{m}$ in reflection configuration. Because of the symmetry of the OuT, the ROI is limited to a 64 pixel wide strip across the y-direction.

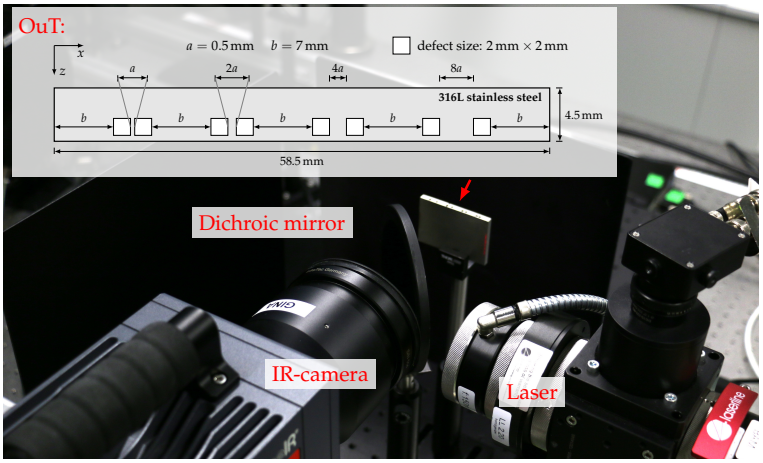

Figure 1. Experimental setup: An OuT containing continuous rectangular channels (defects) is excited using a laser line and a dichroic mirror while a infrared camera records its temperature response.

A dichroic mirror is used to compact the setup and avoid perspective distortion. The OuT is allowed to cool for 40 s between consecutive measurements.

4. Results & Discussion

Calculating the resulting virtual wave fields for all $N_{\mathrm{meas}} = 121$ measurements using a virtual speed of sound of $c = 1$, $\lambda = 0.01$ and $\rho_{\mathrm{ADMM}} = 0.0039$ at a depth discretization of $\Delta_z = 4.5\,\mu\mathrm{m}$ leads to the result shown in Figure 2(**a**). Here, the sum of all virtual wave fields is displayed. The white line indicates the back wall of the OuT at $z = 4.5\,\mathrm{mm}$. In total, depths up to two times the thickness of the OuT have been reconstructed. The result already shows a clear indication of the defects and the wakes in the virtual wave field introduced by them. This mostly affects the area below the defects and directly above them.

Applying the aforedescribed TFM procedure to the virtual wave fields, making full use of all three spatial dimensions, leads to the result shown in Figure 2(**b**). Here, a single slice through the middle of the ROI is shown. Compared to the result of the virtual wave transformation, the defect contrast has clearly improved, and defects are well visible. The defect wakes are somewhat suppressed, but the remains are still visible. Even the smallest defect pair with a gap of 0.5 mm at a depth of 2 mm can be differentiated using this technique.

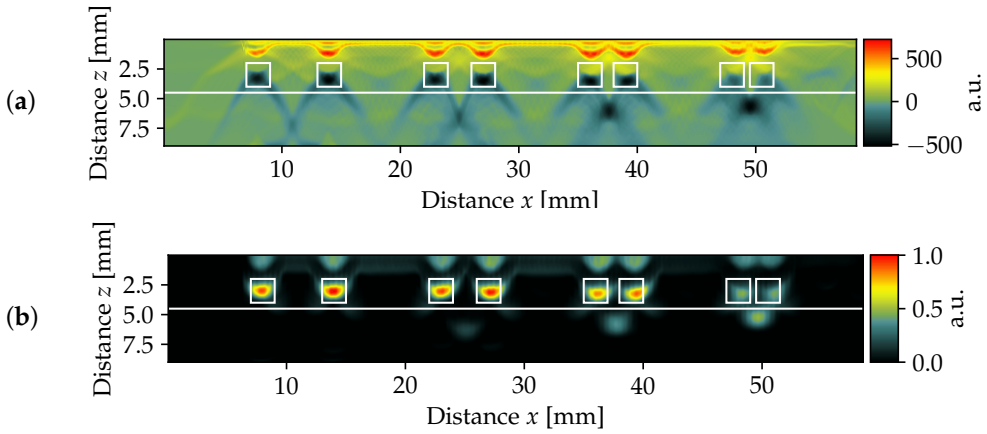

Figure 2. (a) Sum of all $N_{\text{meas}} = 121$ virtual wave transformations using $c = 1$, $\lambda = 0.01$ and $\rho_{\text{ADMM}} = 0.0039$. (b) TFM reconstruction of the OuT. A single slice through the middle of the ROI is shown. The white line indicates the back wall of the OuT.

5. Outlook

The presented results are very promising and show that the combination of multiple measurements with spatially structured laser heating and the application of the TFM in the virtual wave domain is a feasible method for 3D defect reconstruction. Additional measurements using round laser spot step scanning on an OuT with a more complex defect geometry also reinforce this assumption. Due to the limited scope of this manuscript, a more detailed overview is to be published in a follow-up publication.

Author Contributions: Conceptualization, J.L., C.H. and M.Z.; methodology, L.R., J.L. and C.H.; software, L.R. and J.L.; resources, M.Z.; data curation, L.R. and J.L.; writing—original draft preparation, J.L.; writing—review and editing, all; visualization, J.L. and L.R. All authors have read and agreed to the published version of the manuscript.

Funding: This research received no external funding

Data Availability Statement: The raw data supporting the conclusions of this article will be made available by the authors on request.

Conflicts of Interest: The authors declare no conflicts of interest.

References

1. Burgholzer, P.; Thor, M.; Gruber, J.; Mayr, G. Three-dimensional thermographic imaging using a virtual wave concept. *Journal of Applied Physics* **2017**, *121*, 105102. https://doi.org/10.1063/1.4978010.
2. Thummerer, G.; Mayr, G.; Haltmeier, M.; Burgholzer, P. Photoacoustic reconstruction from photothermal measurements including prior information. *Photoacoustics* **2020**, *19*, 100175. https://doi.org/10.1016/j.pacs.2020.100175.
3. Boyd, S. Distributed Optimization and Statistical Learning via the Alternating Direction Method of Multipliers. *Foundations and Trends in Machine Learning* **2010**, *3*, 1–122. https://doi.org/10.1561/2200000016.
4. Holmes, C.; Drinkwater, B.W.; Wilcox, P.D. Post-processing of the full matrix of ultrasonic transmit–receive array data for non-destructive evaluation. *NDT & E International* **2005**, *38*, 701–711. https://doi.org/10.1016/j.ndteint.2005.04.002.
5. Sobczak, M.; Machynia, A.; Dworakowski, Z.; Roemer, J., Experimental Setup for Nondestructive Testing of Composite Structures Using Laser Spot Thermography. In *Advances in Technical Diagnostics II*; Springer Nature Switzerland, 2023; pp. 75–84. https://doi.org/10.1007/978-3-031-31719-4_8.
6. Lecompagnon, J.; Hirsch, P.D.; Rupprecht, C.; Ziegler, M. Nondestructive thermographic detection of internal defects using pixel-pattern based laser excitation and photothermal super resolution reconstruction. *Scientific Reports* **2023**, *13*. https://doi.org/10.1038/s41598-023-30494-2.